Chapter 2

Virtual Synchronous Generator: Modelling, Control and Hardware Developement

2.1 Introdution

This chapter consists of VSG block diagram, control scheme, LCL filter design and small-signal model of VSG. From the small signal model of VSG, parameters of the VSG control is derived. A prototype of VSG is developed and the VSG control is verified through the experimental results. The details of VSG is discussed in the following sections.

2.2 Block diagram of VSG

To implement VSG control, a voltage source inverter is used to mimic the characteristics of a synchronous machine. The power circuit of VSG involves a voltage source inverter, an LC filter and the DC source. A 3-phase VSG hardware circuit is shown in Figure 2.1. The switches of the inverter is operated through PWM pulses. LC filters are connected at the AC terminals of the inverter to reduce the ripples in the output voltage due to switching harmonics. 3-phase inverter is integrated with the distribution grid at the PCC through grid side impedance (L_g,R_g). Inverter side filter comprises inductor (L_s,R_s), capacitor (C_f) and a damping resistor (R_f). Inductors (L_g,R_g) doesn't play any role in the islanded mode operation of VSG since it is not the part of VSG. During grid-connected operation,

grid side inductor plays an important role in synchronization as well as power control.

The VSG control algorithm is implemented in the dSPACE (Digital signal processor). Voltage and current signals such as v_o, i_o, etc. are sensed through voltage and current sensors respectively. These sensed signals are used as a feedback to the micro controller. Inside the controller, feedback voltage and current signals are used to calculte the active and reactive powers. Then, the power, voltage and current values are used for the implementation of VSG algorithm. DSP processor generates the PWM pulses for the IGBT switches of the VSI.

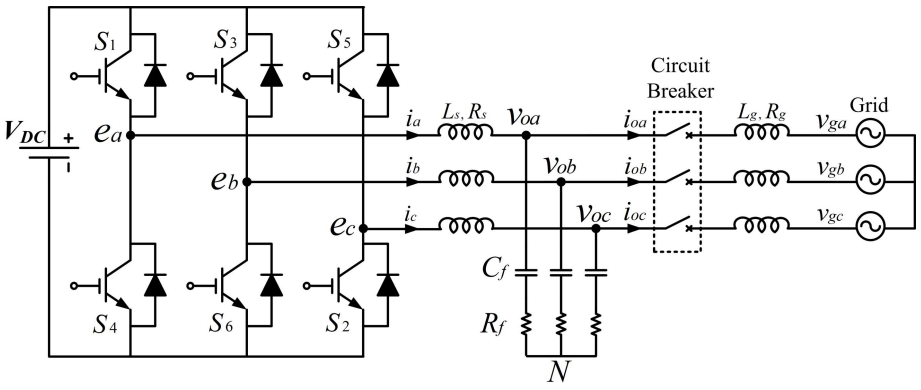

Figure 2.1: Power schematic of VSG

2.3 Control Scheme of VSG

Control algorithm of VSG is derived through the characteristics equation of the SG. Control scheme consists of outer power controler and inner voltage controller. Power control loop consists of active and reactive power loop. Control diagram of VSG is shown in Figure 2.2.

2.3.1 Active Power Control

Active power control is designed based on the swing equation of the synchronous machine as shown in the equation (2.1). The active power loop of the VSG is developed by including virtual inertia for supporting the grid frequency disturbances. This controller is developed by using the mathematical model of a wound rotor synchronous machine. The mechanical dynamic equation of the synchronous machine is given below in equation

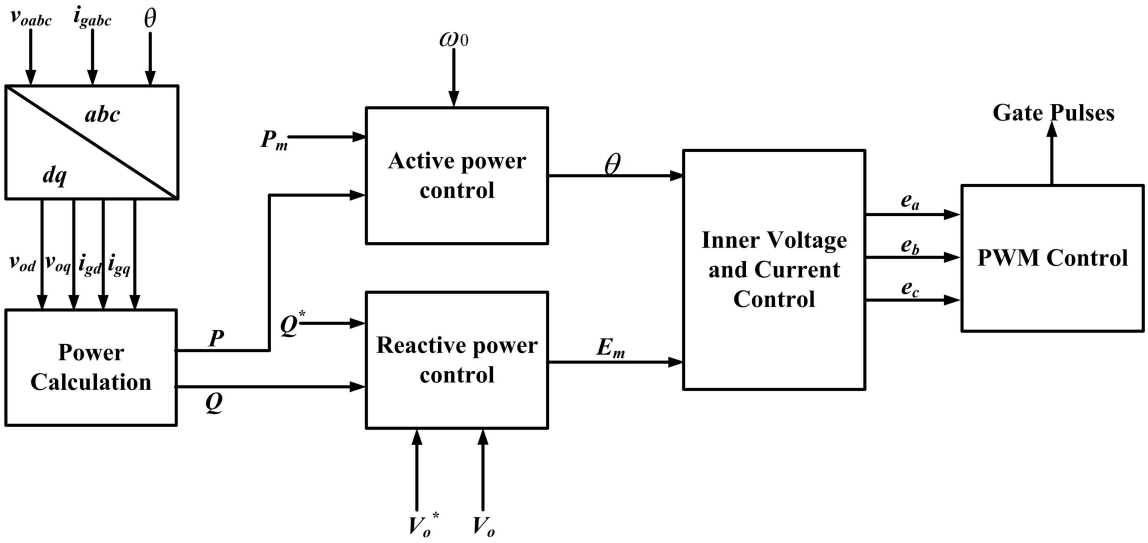

Figure 2.2: Control scheme of VSG

(2.1). Equation (2.1) is modified as equation (2.2) by replacing θ with ω as shown below,

$$J\frac{d^2\theta}{dt^2} = T_m - T_e - D_p\frac{d\theta}{dt} \tag{2.1}$$

$$J\frac{d\omega}{dt} = T_m - T_e - D_p(\omega - \omega_0) \tag{2.2}$$

where J is the moment of inertia, T_m is the input torque, D_p is the damping coefficient, θ is the virtual rotor angle, ω is the rotor angular velocity, ω_{ref} is the grid frequency in rad/sec, and T_e is the generated electrical torque. Here, the number of pole pairs is considered as 1. So, the mechanical speed is the same as the electrical speed.

The input torque (T_m) is calculated from the reference real power (P_m) and the reference angular frequency (ω_0):

$$T_m = \frac{P_m}{\omega_0} \tag{2.3}$$

The electrical torque (T_e) is calculated from the generated real power (P) from the converter and the angular frequency (ω):

$$T_e = \frac{P}{\omega} \tag{2.4}$$

The output active and reactive powers of the VSG can be calculated from the three phase VSG voltages and currents. The power calculation can be conducted in the *abc* frame, $\alpha\beta$ frame, or *dq* frame. Here, three-phase VSG voltages and currents are converted

from *abc* frame to *dq* frame as shown below in the equation (2.5) and equation (2.6), respectively:

$$\begin{bmatrix} v_{od} \\ v_{oq} \\ v_{o0} \end{bmatrix} = \frac{2}{3} \begin{bmatrix} \cos(\omega t) & \cos\left(\omega t - \frac{2\pi}{3}\right) & \cos\left(\omega t + \frac{2\pi}{3}\right) \\ -\sin(\omega t) & -\sin\left(\omega t - \frac{2\pi}{3}\right) & -\sin\left(\omega t + \frac{2\pi}{3}\right) \\ \frac{1}{2} & \frac{1}{2} & \frac{1}{2} \end{bmatrix} \begin{bmatrix} v_{oa} \\ v_{ob} \\ v_{oc} \end{bmatrix} \tag{2.5}$$

$$\begin{bmatrix} i_{gd} \\ i_{gq} \\ i_{g0} \end{bmatrix} = \frac{2}{3} \begin{bmatrix} \cos(\omega t) & \cos\left(\omega t - \frac{2\pi}{3}\right) & \cos\left(\omega t + \frac{2\pi}{3}\right) \\ -\sin(\omega t) & -\sin\left(\omega t - \frac{2\pi}{3}\right) & -\sin\left(\omega t + \frac{2\pi}{3}\right) \\ \frac{1}{2} & \frac{1}{2} & \frac{1}{2} \end{bmatrix} \begin{bmatrix} i_{ga} \\ i_{gb} \\ i_{gc} \end{bmatrix} \tag{2.6}$$

where v_{od}, v_{oq} and v_{o0} are the output voltages of VSG in the $dq0$ frame, and i_{gd}, i_{gq} and i_{g0} are the injected grid currents in the $dq0$ frame. Using equation (2.5) and equation (2.6), the output active and reactive powers of the VSG can be expressed as:

$$P = v_{od} i_{gd} + v_{oq} i_{gq} \tag{2.7}$$

$$Q = v_{oq} i_{gd} - v_{od} i_{gq} \tag{2.8}$$

The output active power P is fed to the active power controller, as shown in the Figure 2.3, to estimate the phase angle of the voltage reference θ, while the output reactive power Q is fed to the reactive power controller to estimate the amplitude of the voltage reference $\sqrt{2}E$. The reference input torque of active power control loop consists

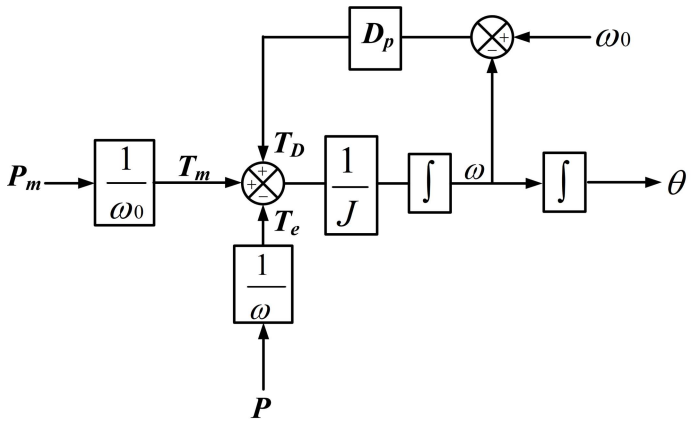

Figure 2.3: Active power control loop of VSG

of mechanical torque T_m and the damping term T_D. T_D is calculated by multiplying the difference between the actual angular frequency of the capacitor voltages ω and the reference angular frequency ω_0 with a damping coefficient D_p. So, total reference torque

$= T_m + D_p(\omega_0 - \omega)$. Since $\omega \approx \omega_g$, the VSG can automatically change its output active power according to the grid frequency, where ω_g is the angular frequency of the grid. Meanwhile, the integral term $1/Js$ is adopted here to introduce the virtual inertia.

2.3.2 Reactive power control

The operating principle of the reactive power controller as shown in the Figure 2.4, is similar to that of the active power controller. The reactive power control loop is used to control the voltage magnitude and reactive power generated by the VSG (Q). The voltage is regulated to the reference value using the voltage droop coefficient (D_q). The actual reactive power generated from the VSG (Q) is calculated using the load voltage and VSG current. The value of k_{iq} is decided from the Q/V droop characteristics [$Q^* = Q + D_q(V_o^* - V_o)$] to participate in the regulation of grid voltage. The peak value (E_m) of the reference voltage (e) is calculated by using the reactive power loop.

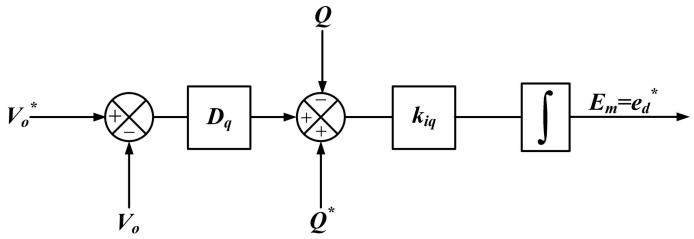

Figure 2.4: Reactive power control loop of VSG

Now we can write the following equation from the reactive power control loop:

$$\sqrt{2}E = k_{iq} \int (Q^* - Q + D_q(V_o^* - V_o))\, dt \tag{2.9}$$

where V_o is the output voltage of the VSG,
V_o^* is the reference output voltage, and E is the RMS reference voltage.

Since $V_o \approx V_g$, the VSG can automatically change its output reactive power according to the grid voltage, where V_g is the root-mean-square (rms) value of the grid voltages. The virtual inertia is embodied by the integral term k_{iq}/s.

So, the power control scheme shown in Figure 2.2 is indeed reproducing the essential behavior of a real SG, including the damping mechanism and the inertial characteristic, which is beneficial to improve the grid stability.

The reference voltages e_{abc} at the load terminals are calculated from the rotor position angle (θ) and peak reference voltage (E_m). Now, this reference voltage is used in the inner voltage controller discussed in the next subsection. For designing the inner voltage and current controller, state equations of the inductor current and the capacitor voltage is derived below.

The output LC filter and the grid-interfacing inductance can be represented with the following state equations by assuming that the inverter ideally produces the demanded inverter bridge voltage [145].

$$\frac{di_d}{dt} = -\frac{1}{L_s}i_d + wi_q + \frac{1}{L_s}e_d - \frac{1}{L_s}v_{od} \tag{2.10}$$

$$\frac{di_q}{dt} = -\frac{1}{L_s}i_q - wi_d + \frac{1}{L_s}e_q - \frac{1}{L_s}v_{oq} \tag{2.11}$$

$$\frac{dv_{od}}{dt} = wv_{oq} + \frac{1}{C_f}i_d - \frac{1}{C_f}i_{od} \tag{2.12}$$

$$\frac{dv_{oq}}{dt} = -wv_{od} + \frac{1}{C_f}i_q - \frac{1}{C_f}i_{oq} \tag{2.13}$$

$$\frac{di_{od}}{dt} = -\frac{1}{L_g}i_{od} + wi_{oq} + \frac{1}{L_g}v_{od} - \frac{1}{L_g}v_{gd} \tag{2.14}$$

$$\frac{di_{oq}}{dt} = -\frac{1}{L_g}i_{oq} - wi_{od} + \frac{1}{L_g}v_{oq} - \frac{1}{L_g}v_{gq} \tag{2.15}$$

2.3.3 Voltage Control

Figure 2.5 shows the voltage controller block diagram including all feedback and feed-forward terms. Output voltage control is achieved with a standard PI controller. The corresponding state equations are given in (2.16)-(2.17), along with the algebraic equations given in (2.18) and (2.19) [145].

$$\frac{d\phi_d}{dt} = e_d^* - v_{od} \tag{2.16}$$

$$\frac{d\phi_q}{dt} = e_q^* - v_{oq} \tag{2.17}$$

$$i_d^* = i_{od} - wC_f v_{oq} + K_{pv}(e_d^* - v_{od}) + K_{iv}\phi_d \tag{2.18}$$

$$i_q^* = i_{oq} + wC_f v_{od} + K_{pv}(e_q^* - v_{oq}) + K_{iv}\phi_d \tag{2.19}$$

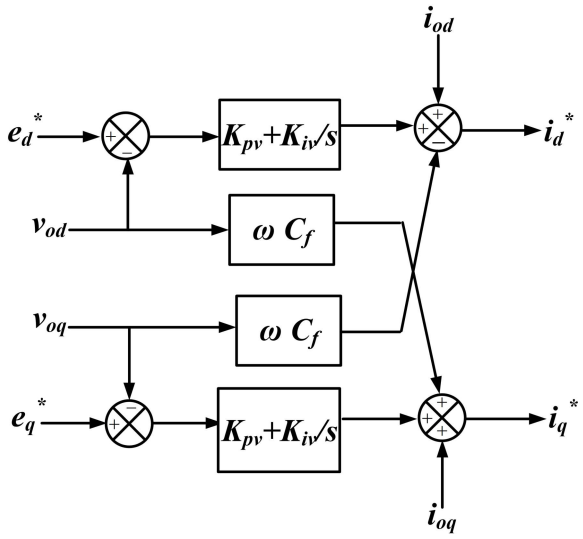

Figure 2.5: Voltage control of VSG

2.3.4 Current Controller

Figure 2.6 shows the current controller structure. Control of the filter inductor current is achieved with a standard PI controller. The corresponding state equations are given in (2.20) along with the algebraic equations given in (2.21) and (2.22).

$$\frac{d\gamma_d}{dt} = i_d, \quad \frac{d\gamma_q}{dt} = i_q \tag{2.20}$$

$$e_d = v_{od} - wL_s i_q + K_{pi}(i_d - i_d^*) + K_{ii}\gamma_d \tag{2.21}$$

$$e_q = v_{oq} + wL_s i_d + K_{pi}(i_q - i_q^*) + K_{ii}\gamma_q \tag{2.22}$$

2.4 Filter Design

Single phase equivalent circuit of LC filter with grid impeadance is shown in Figure 2.7. Where,

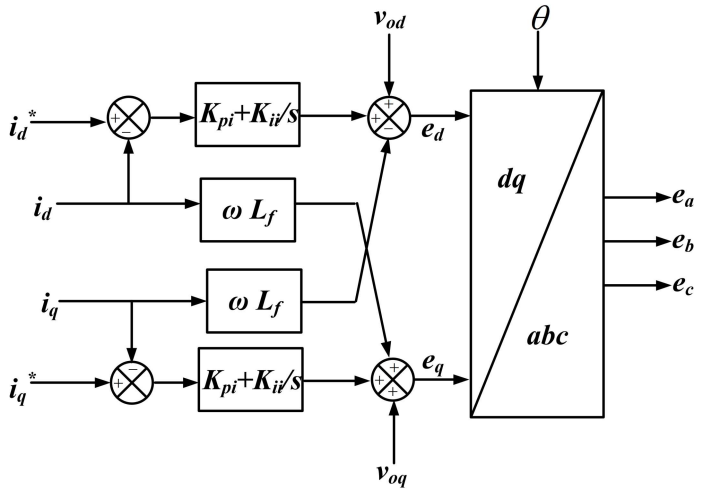

Figure 2.6: Current control of VSG

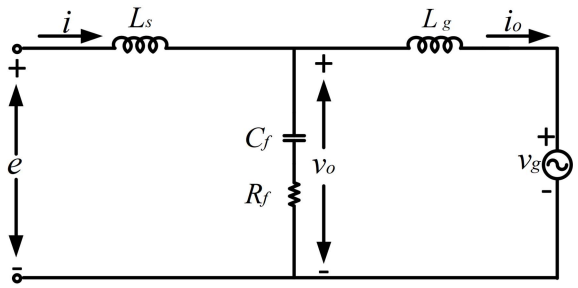

Figure 2.7: Single phase equivalent circuit of filter

e = terminal voltage of inverter.

v_o = output voltage across the capacitor.

v_g = grid voltage

i_o = output current or grid current.

The base values of the quantities are given in Table 2.1.

Here, P_{Base} is the base value of power. V_{Base} and I_{Base} is the base value of output voltage and current, respectively. Similarly, Z_{Base}, L_{Base} and C_{Base} are the base impeadance, base inductance and base capacitance, respectively. ω_{Base} is the base value of frequency in rad/sec and f_{sw} is the switching frequency. Let,

ω_{dom} = dominating frequency = switching frequency = ω_{sw},

ω_r = resonance frequency

ω_{fu} = fundamental frequency

Table 2.1: Base values

S.No.	Quantity	Base Values
1	P_{Base}	5 kW
2	V_{Base}	230 V
3	I_{Base}	22.74 A
4	Z_{Base}	9.68 Ω
5	L_{Base}	30.812 mH
6	C_{Base}	328.83 μF
7	ω_{Base}	$2 * \pi * 50$
8	f_{sw}	10 kHz

Then,

$$Base\ \omega_{dom} = \frac{2\pi * 10000}{2\pi * 50} = 200$$

Transfer function of grid current to inverter output voltage is given by [145]:

$$\frac{I_o(s)}{E(s)} = \frac{1}{s(L_s + L_g)(1 + \frac{s^2 L_s L_g C_f}{L_s + L_g})} \tag{2.23}$$

We assume,

$$L_s + L_g = L \tag{2.24}$$

$$\frac{L_s L_g}{L_s + L_g} = L_P \tag{2.25}$$

$$\omega_r = \frac{1}{\sqrt{L_P C_f}} \tag{2.26}$$

ω_r = resonance frequency in rad/sec. Equations (2.23)-(2.26) are used to design the filter component values.

2.4.1 Components selection procedure

- Choose a resonant frequency ω_r which is well separated from both ω_{fu} and ω_{sw} so that the by-pass paths for the different frequency components of currents are effective. Too low value of ω_r is not desirable as it requires a larger values of L or c or

both.

ω_r is normally chosen as 10 times less than switching frequency which is well separated from fundamental and switching frequency . So,

$$\omega_r = 1000Hz$$

$$\omega_r(pu) = 20$$

- From equation (2.23), the gain of transfer function at $s = j\omega_{dom}$ can be given as:

$$\frac{|I_o(j\omega_{dom}|}{|E(j\omega_{dom})|} = \frac{1}{L|\jmath\omega_{dom}||1 - (\frac{\omega_{dom}}{\omega_r})^2|}$$

Hence, inductance L can be calculated as,

$$L = \frac{|E(j\omega_{dom})|}{|I_o(j\omega_{dom}||\jmath\omega_{dom}||1 - (\frac{\omega_{dom}}{\omega_r})^2|}$$

A limit on the minimum value of inductance can be imposed from grid current at the switching frequency. Hence, compute $L_{min1}(p.u.)$ using the above equation, Put $s = \omega_{dom}$

$$L_{min1} = \frac{|E(j\omega_{dom})|}{|I_o(j\omega_{dom}||\jmath\omega_{dom}||1 - (\frac{\omega_{dom}}{\omega_r})^2|} \tag{2.27}$$

Voltage of the inverter at switching frequency is $e(j\omega_{dom})$=0.9 p.u. Also according to the IEEE standards harmonic distortion of grid current can not be higher than 0.3 % of the total current demand at harmonic order greater than 35.

So, $I_o(j\omega_{dom}) = 0.003 \;\; p.u.$

Putting all values we get,

$$L_{min1} = 0.016 \;\; pu$$

- A limit on the filter capacitor value (C_{fmax}) can be imposed to reduce the reactive power requirement of the capacitor [151].

$$L_{min2} = \frac{4}{\omega_r^2 C_{fmax}} \tag{2.28}$$

Since, the reactive power flowing through the filter capacitor is not allowed more than 20 %, maximum value of capacitor is chosen as :

$$C_{fmax} = 0.2 \;\; pu$$

Now putting this value in eq. (2.28) we get, $L_{min2} = 0.05$ p.u.

- Choose a minimum value of L that satisfies, $L_{min} = max(L_{min1}, L_{min2})$.
  So minimum value of L is chosen as $L_{min} = 0.05$ p.u.

- Choose L_{max}=0.2 p.u. based on dc bus voltage consideration. If we choose higher values of L then higher DC bus voltage will be required, so maximum value of L is constrained by DC bus voltage.

- Now choice of actual L depends on minimizing total power loss. Fundamental loss in the inductor is smaller when we choose L close to L_{min}. But switching loss in the inductor is smaller when we choose L close to L_{max}.
  So Choose a value of L that satisfies,

$$L_{min} \leq L \leq L_{max} \tag{2.29}$$

  We choose $L = 0.11$ p.u.
  Because at this value of L we get the minimum power losses and optimized value of L, C_f & R_f.
  So actual value of L is:

$$L = 0.11 * base\ value$$

$$L = 0.11 * 30.812 * 10^{-}3$$

$$L = 3.38\ \ mH \approx 3.4\ \ mH$$

- Choose $L_s = L_g = L/2$ from the point of view of keeping the cost of inductor to be less.
  So, $L_s = L_g = 1.69\ \ mH \approx 1.7\ \ mH$

- Now actual value of C_f can be calculated as:

$$C_f = \frac{4}{\omega_r^2 L} = \frac{4}{20^2 * 0.11} = 0.09\ \ pu. \tag{2.30}$$

  So actual value of C_f is :

$$C_f = 0.09 * base\ value$$

$$C_f = 0.09 * 328.83 * 10^{-}6$$

$$C_f = 29.6\mu F \approx 30\mu F$$

- Now damping resistor R_f in series with C_f can be calculated as:

$$R_f = \sqrt{\frac{L}{C_f}} \tag{2.31}$$

This value of R_f gives a low value of Quality Factor so that we get the better dynamic response without much oscillations.

$$R_f = \sqrt{\frac{3.38 * 10^{-}3}{30 * 10^{-}6}}$$

$$R_f = 10.6\Omega$$

Check if with the damping components included , the filter gives the required attenuation for the dominant harmonic component. If the attenuation is less, increase L and repeat the same procedure.
So we have calculated all the values of filter as given in table below:

Table 2.2: Filter values

S.No.	Components	Values
1	L	3.4 mH
2	L_s=L_g	1.7 mH
3	C_f	30 μF
4	R_f	10.6 Ω

After putting all the values in the equation (2.23), the transfer function of grid current to inverter voltage can be estimated. The bode plot of grid current to inverter voltage transfer function $I_g(s)/E(s)$ is shown in the Figure 2.8. From the bode plot, it is clear that both the gain margin and phase margin of the transfer function is within the stability margin. Gain margin is around 22.22 dB and phase margin is 90^0. Also, the gain at the switching frequency is very low. Hence, the designed filter provides enough attenuation at the switching frequency.

2.5 Small Signal Modelling of VSG

To properly design the control parameters of VSG, small signal analysis of the VSG is needed. This section presents the small signal modelling of VSG. Initially, transfer

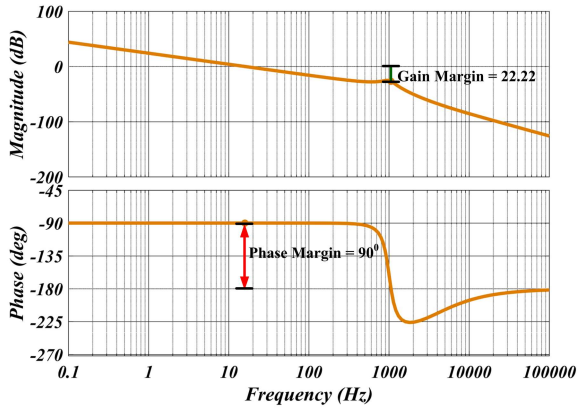

Figure 2.8: Bode plot of grid current to inverter voltage transfer function $I_g(s)/e(s)$

function of both active and reactive power control is derived. Then, paramaters of the VSG is calculated by using the small signal transfer function of VSG. Complete small signal analysis is discussed in the following subsections.

2.5.1 Transfer function of active and reactive power of VSG

The phasor representations of the sinusoidal voltage and current can be used to calculate the active and reactive powers, when the three-phase grid voltages are balanced. $\overline{V_g} = V_g\angle 0$ and $\overline{V_o} = V_o\angle\delta$ can be used to represent the phasors of the grid voltages and the capacitor voltages, respectively, where δ is the power angle, which is expressed as

$$\delta = \theta - \theta_g \tag{2.32}$$

Where, θ = phase of the output voltage, θ_g = grid voltage phase

The grid impedance can be represented by $Z_g = R_g + jX_g$, where R_g denotes the resistive component, while X_g denotes the inductive component. On that basis, the phasor of the injected grid currents can be written as

$$S = 3\overline{V_o}\ \overline{I_g^*} \tag{2.33}$$

$$S = 3\overline{V_o}(\frac{\overline{V_o} - \overline{V_g}}{R_g - jX_g}) \tag{2.34}$$

$$S = \frac{3V_o^2}{R_g - jX_g} - \frac{3V_oV_g}{R_g - jX_g}(\cos\delta + j\sin\delta) \tag{2.35}$$

It is assumed that the grid impedance Z_g is mainly inductive. So

$$S = \frac{3V_oV_g \sin\delta}{X_g} + j\frac{3V_o^2}{X_g} - j\frac{3V_oV_g \cos\delta}{X_g} \tag{2.36}$$

$$S = \frac{3V_oV_g \sin\delta}{X_g} + j\frac{3V_o}{X_g}(V_o - V_g \cos\delta) \tag{2.37}$$

$$S = P + jQ \tag{2.38}$$

So P and Q can be written as:

$$P = \frac{3V_oV_g \sin\delta}{X_g} \tag{2.39}$$

$$Q = \frac{3V_o}{X_g}(V_o - V_g \cos\delta) \tag{2.40}$$

This is the average value of active and reactive power. Now for deriving small signal model, we apply perturbations to the active and reactive power. Let,

$$x = x_n + \hat{x}$$

Where x is the large signal value of any quantity , x_n is the steady state value and $\hat{x}$ is the small ac variation from the steady state value.

$$\omega = \omega_n + \hat{\omega} \tag{2.41}$$

$$\delta = \delta_n + \hat{\delta} \tag{2.42}$$

$$\omega_0 = \omega_n + \hat{\omega_0} \tag{2.43}$$

$$V_o = V_{on} + \hat{V_o} \tag{2.44}$$

$$V_o^* = V_{on} + \hat{V_o^*} \tag{2.45}$$

$$V_g = V_{gn} + \hat{V_g} \tag{2.46}$$

$$P = P_n + \hat{P} \tag{2.47}$$

$$Q = Q_n + \hat{Q} \tag{2.48}$$

$$P_m = P_n + \hat{P_m} \tag{2.49}$$

$$Q^* = Q_n + \hat{Q^*} \tag{2.50}$$

$$T_m = T_{mn} + \hat{T_m} \tag{2.51}$$

$$T_e = T_{en} + \hat{T_e} \tag{2.52}$$

2.5.2 Derivation of Active Power Transfer function

Active power P is derived as:

$$P = \frac{3V_oV_g \sin\delta}{X_g}$$

$$T_e\omega = \frac{3V_oV_g \sin\delta}{X_g} \tag{2.53}$$

By applying above perturbations in active power equation we get

$$(T_{en} + \hat{T}_e)(\omega_n + \hat{\omega}) = \frac{3(V_{on} + \hat{V}_o)(V_{gn} + \hat{V}_g)\sin(\delta_n + \hat{\delta})}{X_g} \tag{2.54}$$

$$(T_{en}\omega_n + T_{en}\hat{\omega} + \hat{T}_e\omega_n + \hat{T}_e\hat{\omega}) = \frac{3(V_{on} + \hat{V}_o)(V_{gn} + \hat{V}_g)(\sin\delta_n\cos\hat{\delta} + \cos\delta_n\sin\hat{\delta})}{X_g} \tag{2.55}$$

Since $\hat{\delta}$ is very small:

$$\sin\hat{\delta} \approx \hat{\delta} \text{ and } \sin\delta_n \approx \delta_n$$
$$\cos\hat{\delta} \approx 1 \text{ and } \cos\delta_n \approx 1$$

$$(T_{en}\omega_n + T_{en}\hat{\omega} + \hat{T}_e\omega_n + \hat{T}_e\hat{\omega}) = \frac{3V_{on}V_{gn} + 3V_{on}\hat{V}_g + 3\hat{V}_oV_{gn} + 3\hat{V}_o\hat{V}_g\delta_n + \hat{\delta}}{X_g} \tag{2.56}$$

$$= \frac{3V_{on}V_{gn}\delta_n}{X_g} + \frac{3V_{on}V_{gn}\hat{\delta}}{X_g} + \frac{3V_{on}\hat{V}_g\delta_n}{X_g} + \frac{3V_{on}\hat{V}_g\hat{\delta}}{X_g} + \frac{3\hat{V}_oV_{gn}\delta_n}{X_g} + \frac{3\hat{V}_oV_{gn}\hat{\delta}}{X_g} + \frac{3\hat{V}_o\hat{V}_g\delta_n}{X_g} + \frac{3\hat{V}_o\hat{V}_g\hat{\delta}}{X_g} \tag{2.57}$$

Now the product of two small AC variations will be very small. So neglect all quantities with the product of small signals and DC quantities.

$$T_{en}\hat{\omega} + \hat{T}_e\omega_n = \frac{3V_{on}V_{gn}\hat{\delta}}{X_g} + \frac{3V_{gn}\delta_n(\hat{V}_o + \hat{V}_g)}{X_g} \tag{2.58}$$

For deriving the open-loop transfer function of active power $\hat{T}_e$ to angle $\hat{\delta}$ apply Laplace transform and set all other perturbations to zero.

$$\hat{T}_e(s)\hat{\delta}(s) = \frac{3V_{on}V_{gn}}{X_g\omega_n} \tag{2.59}$$

2.5.3 Derivation of Reactive Power Transfer Function

By applying above perturbations in reactive power equation we get

$$Q_n + \hat{Q} = \frac{3(V_{on} + \hat{V}_o)X_g(V_{on} + \hat{V}_o - (V_{gn} + \hat{V}_g)\cos(\delta_n + \hat{\delta}))}{X_g} \tag{2.60}$$

$$= \frac{3(V_{on} + \hat{V}_o)X_g(V_{on} + \hat{V}_o - V_{gn} + \hat{V}_g(\cos\delta_n\cos\hat{\delta} - \sin\delta_n\sin\hat{\delta}))}{X_g} \tag{2.61}$$

Since $\hat{\delta}$ is very small $\sin\hat{\delta} \approx \hat{\delta}$ and $\sin\delta_n \approx \delta_n$, also $\cos\hat{\delta} \approx 1$ and $\cos\delta_n \approx 1$

$$Q_n + \hat{Q} = \frac{3(V_{on} + \hat{V}_o)X_g(V_{on} + \hat{V}_o - V_{gn} + \hat{V}_g - \delta_n\hat{\delta})}{X_g} \tag{2.62}$$

$$= \frac{3V_{on}V_{on}}{X_g} - \frac{3V_{on}V_{gn}}{X_g} + \frac{3V_{on}\hat{V}_o}{X_g} - \frac{3\hat{V}_oV_{gn}}{X_g} + \frac{3V_{on}\hat{V}_g}{X_g} - \frac{3V_{gn}\hat{V}_g}{X_g} \tag{2.63}$$

Now the product of two small AC variations will be very small. So neglect all quantities with the product of small signals and DC quantities.

$$\hat{Q} = \frac{3V_{on}\hat{V}_o}{X_g} + \frac{3V_{on}\hat{V}_g}{X_g} - \frac{3V_{on}V_{gn}}{X_g} \tag{2.64}$$

$$= \frac{3\hat{V}_o\hat{V}_g}{X_g} - \frac{3V_{on}\hat{V}_g}{X_g} \tag{2.65}$$

For deriving the open loop transfer function of reactive power Q to angle δ apply Laplace transform and set all other perturbation to zero.

$$\frac{\hat{Q}(s)}{\left(\hat{V}_o(s) - \hat{V}_g(s)\right)} = \frac{3V_{on}}{X_g} \tag{2.66}$$

2.5.4 Transfer Function of Active Power Controller

Now, by applying the perturbation to the swing equation (2.2), we have:

$$J\frac{d(\omega_n + \hat{\omega})}{dt} = (T_{mn} + \hat{T}_m) - (T_{en} + \hat{T}_e) - D_p\left[(\omega_n + \hat{\omega}) - (\omega_n + \hat{\omega_0})\right] \tag{2.67}$$

$$J\frac{d\omega_n}{dt} + J\frac{d\hat{\omega}}{dt} = (T_{mn} - T_{en}) + (\hat{T}_m - \hat{T}_e) - D_p\left[(\omega_n + \hat{\omega}) - (\omega_n + \hat{\omega_0})\right] \tag{2.68}$$

Neglecting all DC quantities, we have:

$$J\frac{d\hat{\omega}}{dt} = (\hat{T}_m - \hat{T}_e) - D_p(\hat{\omega} - \hat{\omega_0}) \tag{2.69}$$

Taking the Laplace transform:

$$Js\hat{\omega}(s) = (\hat{T}_m(s) - \hat{T}_e(s)) - D_p\hat{\omega}(s) \tag{2.70}$$

$$\hat{T}_m(s) - \hat{T}_e(s) = Js\hat{\omega}(s) + D_p\hat{\omega}(s) \tag{2.71}$$

$$\frac{\hat{\omega}(s)}{\hat{T}_m(s) - \hat{T}_e(s)} = \frac{1}{Js + D_p} \tag{2.72}$$

This is the active power controller transfer function.

2.5.5 Transfer Function of Reactive Power Controller

For deriving the small signal model, we apply perturbation in the above equation (2.7). Then,

$$\sqrt{2}(E_n + \hat{E}) = k_{iq} \int \left((Q_n + \hat{Q}^*) - (Q_n + \hat{Q}) + \sqrt{2}D_q(V_{on} + \hat{V}_o^* - (V_{on} + \hat{V}_o)) \right) dt \tag{2.73}$$

Neglecting all DC quantities, we have:

$$\sqrt{2}\hat{E} = k_{iq} \int \left(\hat{Q}^* - \hat{Q} + \sqrt{2}D_q(\hat{V}_o^* - \hat{V}_o) \right) dt \tag{2.74}$$

Applying the Laplace transform to the equation, we have:

$$\frac{\sqrt{2}\hat{E}(s)}{k_{iq}} = \hat{Q}^*(s) - \hat{Q}(s) + \sqrt{2}D_q(\hat{V}_o^*(s) - \hat{V}_o(s)) \tag{2.75}$$

Now, variation in reference voltage is almost negligible. With properly designed capacitor voltage control loop, the capacitor voltages can accurately track the voltage references. So,

$$V_o \approx E$$

So by applying perturbation also,

$$\hat{V}_o(s) \approx \hat{E}(s)$$

Putting this in the above equation, we have:

$$\frac{\sqrt{2}\hat{E}(s)}{k_{iq}} = \hat{Q}^*(s) - \hat{Q}(s) - \sqrt{2}D_q\hat{E}(s) \tag{2.76}$$

By solving this equation we get:

$$\hat{E}(s) = \frac{k_{iq}}{\sqrt{2}} \frac{\left[\hat{Q}^*(s) - \hat{Q}(s)\right]}{s + D_q k_{iq}} \tag{2.77}$$

$$\frac{\hat{E}(s)}{\left[\hat{Q}^*(s) - \hat{Q}(s)\right]} = \frac{k_{iq}}{\sqrt{2}} (\frac{1}{s + D_q k_{iq}}) \tag{2.78}$$

This is the open loop transfer function of the reactive power controller.

2.6 Parameter design of power loop of VSG

This sections discusses about the parameter design of the VSG control. Parameter design of the active and reactive power control is given below in the following sections.

2.6.1 Active Power Loop (APL)

The loop gain of the active power loop can be expressed as:

$$T_p(s) = \frac{3V_{on}V_{gn}}{\omega_n X_g} \cdot \frac{1}{Js + D_p} \cdot \frac{1}{s}$$

$$T_p(s) = \frac{3V_{on}V_{gn}}{\omega_n X_g} \cdot \frac{1}{D_p} \cdot \frac{1}{\left(\frac{s}{D_p/J} + 1\right)} \cdot \frac{1}{s} \tag{2.79}$$

There are two parameters that need to be calculated in APL, which are the integral coefficient J and droop coefficient D_p. D_p is decided by grid code, so only J needs to be determined for ensuring system stability and meeting the requirements of attenuating the double line frequency ripple (DLFR) in APL. The corner frequency of the first order low pass filter in APL is:

$$f_{pL} = \frac{D_p}{2\pi J} \tag{2.80}$$

A higher J results in a lower f_{pL}, which means better attenuation ability of DLFR. But when f_{pL} decreases, the phase lag introduced by the filter increases, which means the phase margin of APL reduces. So there is a limit in choosing J. The magnitude of APL loop gain at cross-over frequency f_{pc} is unity:

$$|T_p(s)| = |T_p(j2\pi f_{pc})| = \frac{3V_{on}V_{gn}}{\omega_n X_g D_p} \cdot \frac{1}{\left|\frac{j2\pi f_{pc}}{D_p/J} + 1\right|} \cdot \frac{1}{|j2\pi f_{pc}|} = 1 \tag{2.81}$$

$$\frac{1}{J} = \frac{2\pi f_{pc}}{D_p}\sqrt{\left(\frac{3V_{on}V_{gn}}{2\pi f_{pc}X_g\omega_n D_p}\right)^2 - 1} \tag{2.82}$$

$$J = \frac{D_p\sqrt{\left(\frac{3V_{on}V_{gn}}{2\pi f_{pc}X_g\omega_n D_p}\right)^2 - 1}}{2\pi f_{pc}} \tag{2.83}$$

Now loop gain of APL loop at $2f_{line}$ can be expressed as:

$$|T_p(j2\pi \cdot 2f_{line})| = \frac{3V_{on}V_{gn}}{\omega_n X_g D_p} \cdot \frac{1}{\left|\frac{j4\pi f_{line}}{D_p/J} + 1\right|} \cdot \frac{1}{|j4\pi f_{line}|} \tag{2.84}$$

Since f_{pL} should be far below than $2f_{line}$ to ensure the DLFR attenuation, the following approximation can be satisfied:

$$\frac{1}{\left|\frac{j4\pi f_{line}}{D_p/J} + 1\right|} \approx \frac{1}{\left|\frac{j4\pi f_{line}}{D_p/J}\right|} \tag{2.85}$$

Now putting this value in above equation we get:

$$|T_p(j2\pi \cdot 2f_{line})| = \frac{3V_{on}V_{gn}}{16\pi^2 f_{line}^2 X_g\omega_n J} \tag{2.86}$$

To attenuate the DLFR in APL, the APL must have sufficiently small loop gain at $2f_{line}$. Let us assume that the loop gain requirement at $2f_{line}$ is a_p. Then to attenuate the DLFR in APL:

$$|T_p(j2\pi \cdot 2f_{line})| \leq a_p \tag{2.87}$$

From equation (2.86):

$$\frac{1}{J} \leq \frac{16\pi^2 f_{line}^2 X_g\omega_n a_p}{3V_{on}V_{gn}} \tag{2.88}$$

$$J \geq \frac{3V_{on}V_{gn}}{16\pi^2 f_{line}^2 X_g\omega_n a_p} = J_{min} \tag{2.89}$$

This is the minimum value of J. So the lower limit of J is constrained by DLFR. To meet the phase margin requirement, the following condition is satisfied:

$$\text{P.M.} = 180^\circ + \text{phase of } T_p \text{ at } f_{pc} \geq \text{PM}_{req} \tag{2.90}$$

So,

$$90^\circ - \tan^{-1}\left(\frac{2\pi f_{pc}}{D_p/J}\right) \geq \text{PM}_{req} \tag{2.91}$$

$$\frac{1}{J} \geq \frac{2\pi f_{pc}}{D_p} \tan(\text{PM}_{req}) \tag{2.92}$$

$$J \leq \frac{D_p}{2\pi f_{pc} \tan(\text{PM}_{req})} = J_{max} \tag{2.93}$$

This is the maximum value of J. So, the upper limit of J is constrained by phase margin criteria.

Specifications

1. Phase margin should be between $30° - 70°$ for better dynamic response of the system.
2. For attenuation of double line frequency ripple in APL, loop gain at $2f_{line}$, $a_p \leq 0.1$.

Design

1. **Droop Coefficient (D_p)**: D_p is determined based on the grid code. It is required that the change of 100% active power corresponds to the change of 2% grid frequency.

$$D_p = \frac{\Delta T_{max}}{\Delta \omega_{max}} = \frac{10000}{2\pi \cdot 50 \cdot 0.02} = 5.07 \tag{2.94}$$

2. **Integral Coefficient (J)**: For better attenuation of DLFR we take $a_p = 0.1$ and $\text{PM}_{req} = 30° - 70°$.

   From equation (2.89):

$$J = \frac{3 \times 220 \times 220}{16\pi^2 \times 50^2 \times 2\pi \times 50 \times 1.2 \times 10^{-3} \times 0.1} \tag{2.95}$$

$$J = 0.031 \approx 0.03 = J_{min} \tag{2.96}$$

   From equation (2.83):

$$0.031 = \frac{5.07\sqrt{\left(\frac{3\times220\times220}{2\pi\times f_{pc}\times 2\pi\times50\times1.2\times10^{-3}\times5.07}\right)^2 - 1}}{2\pi f_{pc}} \tag{2.97}$$

$$f_{pc} = 26.8175 \approx 26.82 \text{ Hz} = f_{pcmax} \tag{2.98}$$

For the maximum value of J, we choose a phase margin of 30°. Then from equation (2.93):

$$J_{max} = \frac{2\pi \times f_{pc}}{5.07 \tan 30^\circ} \tag{2.99}$$

$$J_{max} = \frac{1.3976}{f_{pcmin}} \tag{2.100}$$

Putting this value in equation (2.83) we get:

$$\frac{1.3976}{f_{pcmin}} = \frac{5.07\sqrt{\left(\frac{3\times220\times220}{2\pi\times f_{pcmin}\times2\pi\times50\times1.2\times10^{-3}\times5.07}\right)^2 - 1}}{2\pi f_{pcmin}} \tag{2.101}$$

$$f_{pcmin} = 19.2427 \text{ Hz} \approx 19.24 \text{ Hz} \tag{2.102}$$

Hence,

$$J_{max} = 0.07262 \approx 0.07 \tag{2.103}$$

We have $J_{min} = 0.03$ and $J_{max} = 0.07$, so we have to choose the value of J between 0.03 and 0.07.

From equation (2.83) if we calculate J for various values of f_{pc}, then we can write all these values in a tabular form and we can also plot the graph between J & f_{pc}. Some of the values of J according to f_{pc} are given in the table as follows:

For $J = 0.03$ to $J = 0.07$, we can choose any frequency between 19 Hz to 25 Hz. We choose the crossover frequency as 22 Hz in between 19 Hz and 25 Hz. Hence, the value of $f_{pc} = 22$ Hz so that both DLFR attenuation and phase margin requirements are met:

$$f_{pc} = 22 \text{ Hz} \tag{2.104}$$

By putting this value in equation (2.83) we get:

$$J = \frac{5.07\sqrt{\left(\frac{3\times220\times220}{2\pi\times22\times2\pi\times50\times1.2\times10^{-3}\times5.07}\right)^2 - 1}}{2\pi \times 22} \tag{2.105}$$

$$J = 0.0526 \approx 0.05 \tag{2.106}$$

Table 2.3: Values of J according to f_{pc}

S. No.	Crossover frequency f_{pc} (Hz)	Inertia J
1	10	0.2998
2	11	0.2459
3	12	0.2049
4	13	0.1729
5	14	0.1475
6	15	0.1271
7	16	0.1103
8	17	0.0964
9	18	0.0847
10	19	0.0748
11	20	0.0663
12	21	0.0590
13	22	0.0526
14	23	0.0470
15	24	0.0421
16	25	0.0377

Put the value of J in equation (2.93) we get:

$$0.05 = \frac{5.07}{2\pi \times 22 \tan(\mathrm{PM}_{req})} \tag{2.107}$$

$$\mathrm{PM}_{req} = 34.86^{\circ} \tag{2.108}$$

Now we can calculate the loop gain of APL at $2f_{line}$. From equation (2.86), the loop gain of APL at $2f_{line}$ is:

$$|T_p(j2\pi \cdot 2f_{line})| = \frac{3 \times 220 \times 220}{16\pi^2 \times 50^2 \times 2\pi \times 50 \times 1.2 \times 10^{-3} \times 0.0526} \tag{2.109}$$

$$|T_p(j2\pi \cdot 2f_{line})| = 0.059 = -24.577 \text{ dB} \tag{2.110}$$

We calculated f_{pc} = 22 Hz. Phase margin is 34.86°. Loop gain at $2f_{line}$ is -24.577 dB, which means DLFR is well attenuated. So all the specifications are met as required. Bode plot of APL of VSG is shown in Figure 2.9.

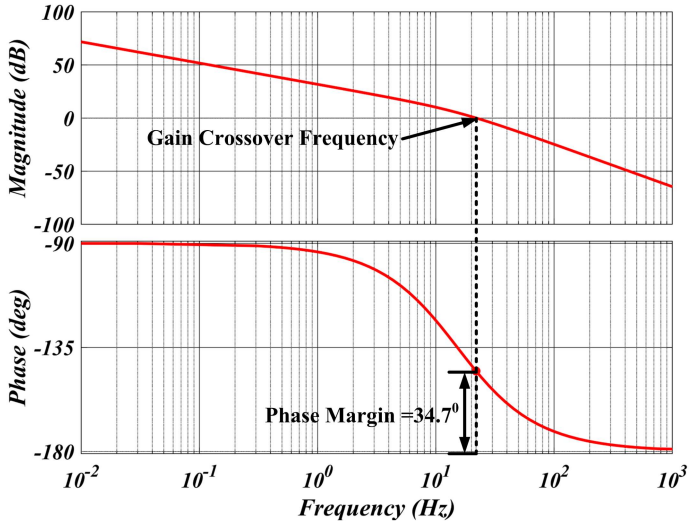

Figure 2.9: Bode magnitude and phase plot of APL of VSG

2.6.2 Reactive Power Loop (RPL)

The loop gain of the reactive power loop is expressed as:

$$T_q(s) = \frac{3V_{on}}{X_g\sqrt{2}D_q} \cdot \frac{1}{\left(\frac{1}{D_q k_{iq}}s + 1\right)} \tag{2.111}$$

There are two parameters that need to be calculated in the RPL: the integral coefficient k_{iq} and the droop coefficient D_q. D_q is decided by the grid code, so only k_{iq} needs to be determined to ensure system stability and meet the requirements of attenuating the double line frequency ripple (DLFR) in the RPL. The corner frequency of the first-order low-pass filter in the RPL is:

$$f_{qL} = \frac{D_q k_{iq}}{2\pi} \tag{2.112}$$

f_{qL} decreases with decreasing k_{iq}, which means better DLFR attenuation, a reduced phase margin, and a slower dynamic response. So k_{iq} should be chosen accordingly. There is only a first-order low-pass filter in the RPL, so the maximum phase-lag introduced by this filter is $-90°$. Hence, the phase margin requirement is always satisfied; only the requirement of DLFR attenuation needs to be considered.

The magnitude of the RPL loop gain at cross-over frequency f_{qc} is unity:

$$|T_q(s)|= |T_q(j2\pi f_{qc})|= \frac{3V_{on}}{X_g\sqrt{2}D_q} \cdot \frac{1}{\left|\frac{j2\pi f_{qc}}{D_q k_{iq}} + 1\right|} = 1 \tag{2.113}$$

So,

$$k_{iq} = \frac{2\pi f_{qc}}{D_q\sqrt{\left(\frac{3V_{on}}{\sqrt{2}X_g D_q}\right)^2 - 1}} \tag{2.114}$$

The magnitude of the RPL loop gain at $2f_{line}$ is expressed as:

$$|T_q(j2\pi \cdot 2f_{line})|= \frac{3V_{on}}{\sqrt{2}X_g D_q} \cdot \frac{1}{\left|\frac{j4\pi f_{line}}{D_q k_{iq}} + 1\right|} \tag{2.115}$$

Since f_{qL} is far below the double line frequency $2f_{line}$ to ensure DLFR attenuation, the following approximation can be satisfied:

$$\frac{1}{\left|\frac{j4\pi f_{line}}{D_q k_{iq}} + 1\right|} \approx \frac{1}{\left|\frac{j4\pi f_{line}}{D_q k_{iq}}\right|} \tag{2.116}$$

By substituting this value into the previous equation, we get:

$$|T_q(j2\pi \cdot 2f_{line})|= \frac{3V_{on}k_{iq}}{4\sqrt{2}\pi f_{line}X_g} \tag{2.117}$$

To attenuate the DLFR in the RPL loop, the RPL loop must have a sufficiently small loop gain at $2f_{line}$. Let us assume that the loop gain requirement at $2f_{line}$ is a_q. Then, to attenuate the DLFR in the RPL:

$$|T_q(j2\pi \cdot 2f_{line})|\leq a_q \tag{2.118}$$

So we have:

$$k_{iq} \leq \frac{4\sqrt{2}\pi f_{line}X_g a_q}{3V_{on}} = k_{iq_{max}} \tag{2.119}$$

This is the upper limit of k_{iq} constrained by DLFR in the RPL. There is no lower limit of k_{iq} since the phase margin requirement of the RPL loop is always satisfied. However, f_{qL} decreases with k_{iq}, which affects the dynamic performance of the system, so k_{iq} should not be too small. Practically, we choose k_{iq} slightly smaller than $k_{iq_{max}}$ to ensure good attenuation and dynamic performance.

The phase margin of the RPL is expressed as:

$$P.M. = 180^\circ + \text{phase of } T_q \text{ at } f_{qc} \tag{2.120}$$

$$P.M. = 180^\circ - \tan^{-1}\left(\frac{2\pi f_{qc}}{D_q k_{iq}}\right) \tag{2.121}$$

Specifications

1. Phase margin should be between $30° - 70°$ for better dynamic response of the system.
2. For attenuation of double line frequency ripple in RPL, the loop gain at $2f_{line}$, $a_q \leq 0.1$.

Design

1. **Droop Coefficient (D_q):** D_q is determined based on the grid code. It is required that 100 % reactive power corresponds to a change of 10 % grid voltage, so:

$$D_q = \frac{\Delta Q}{\Delta V} = \frac{10000}{(220\sqrt{2}) \cdot 10\%} = 321 \tag{2.122}$$

2. **Integral Coefficient (k_{iq}):** For better attenuation of DLFR we take $a_q = 0.1$. So from equation (2.117):

$$k_{iq} = \frac{4\sqrt{2}\pi \cdot 50 \cdot 1.2 \times 10^{-3} \cdot 0.1}{3 \cdot 220} = 0.051 = k_{iq_{max}} \tag{2.123}$$

This is the maximum value of k_{iq}, so k_{iq} should be slightly less than $k_{iq_{max}}$. We choose $k_{iq} = 0.045$. Using this value of k_{iq}, we can calculate the crossover frequency f_{qc} using equation (2.114):

$$0.045 = \frac{2\pi f_{qc}}{321\sqrt{\left(\frac{3 \cdot 220}{\sqrt{2} \cdot 1.2 \times 10^{-3} \cdot 321}\right)^2 - 1}} \tag{2.124}$$

$$f_{qc} = 8.6\,\text{Hz} \tag{2.125}$$

3. **Phase Margin of RPL:**

$$P.M. = 180° - \tan^{-1}\left(\frac{2\pi \cdot 8.6}{321 \cdot 0.045}\right) \tag{2.126}$$

$$P.M. \approx 105° \tag{2.127}$$

4. **Loop Gain at $2f_{line}$:**

$$|T_q(j2\pi \cdot 2f_{line})| = \frac{3 \cdot 220 \cdot 0.045}{4\sqrt{2}\pi \cdot 50 \cdot 2\pi \cdot 1.2 \times 10^{-3}} \tag{2.128}$$

$$|T_q(j2\pi \cdot 2f_{line})| = 0.0886 \approx -21.05\,\text{dB} \tag{2.129}$$

We calculated $f_{qc} = 8.6\,\text{Hz}$. The phase margin is 105°. The loop gain at $2f_{line}$ is -21.05 dB, which means DLFR is well attenuated. So all the specifications are met as required. Bode plot of RPL of VSG is shown in Figure 2.10.

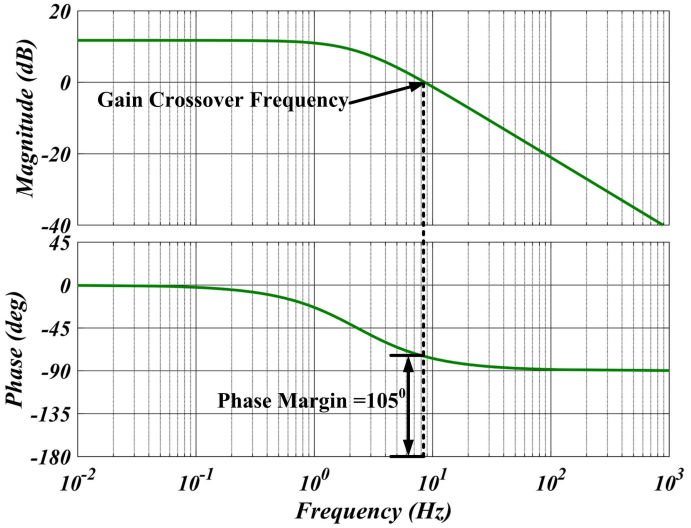

Figure 2.10: Bode magnitude and phase plot of RPL of VSG

2.7 Hardware Development

2.7.1 Hardware Components

Fig. 2.11 shows the developed prototype of a Virtual Synchronous Generator. A 1 kW three phase voltage source inverter is used for implementing grid-connected VSG. Grid voltages (v_{gab}, v_{gbc} and v_{gca}), grid currents (i_{ga}, i_{gb} and i_{gc}), VSG voltages (v_{oab}, v_{obc} and v_{oca}) and VSG currents (i_{oa},i_{ob} and i_{oc}) are sensed using Hall-effect voltage and current sensors respectively.

Microlab Box dSPACE dS1202 is used as a controller for controlling the prototype VSG in real time. The prototype of the VSG mainly consists of an inverter, DS1202 microcontroller, and BESS as shown in Fig. 2.11. Interfacing circuits for voltage and current sensors, and opto-coupler used in this experimental system are discussed in detail in the following section.

2.7.2 Signal Conditioning Circuit for Hall Effect Voltage Sensors

VSG voltages and grid voltages are sensed using voltage sensors (LEM voltage sensors, LV25P) and these signals are converted to ±10 V range, which is the maximum ADC voltage of the dSPACE DS1202 processor. Inside the processor, these analog signals are

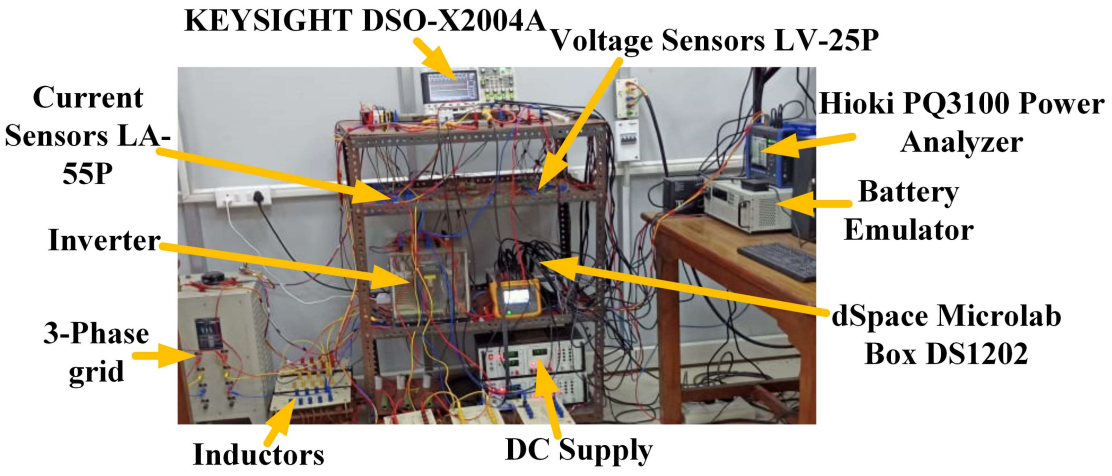

Figure 2.11: Hardware prototype of virtual synchronous generator

converted into digital signals using an analog to digital converter (ADC) and then scaled up to the actual level inside the processor. The interfacing circuit for converting the sensed voltage into ADC voltage range is shown in Figure 2.12.

The line voltage rating of the VSG is 230 V rms. Therefore, the peak voltage is 325.269 V. According to the data sheet of the voltage sensor (LV25P), the primary nominal rms current is 10 mA. Therefore, input resistance R_{in} is selected as 23 kΩ (325.269/10 mA × $\sqrt{2}$). The power rating of the input resistor is 2.3 W (230^2/23 kΩ).

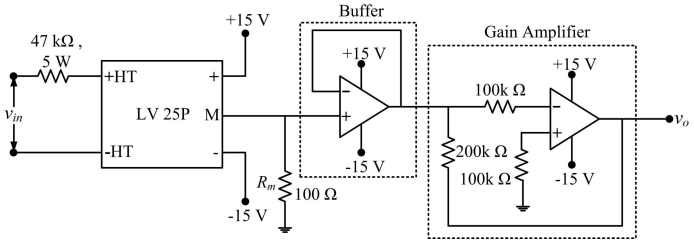

Figure 2.12: Interfacing circuit for voltage sensor LV 25P

According to availability and taking the margin, input resistance (R_{in}) is selected as 47kΩ, 5W. According to the LV25P data sheet, secondary nominal rms current is 25 mA. Minimum and maximum resistances according to the data sheet are given as 100 Ω and 350 Ω. Measuring resistance R_m is selected as 100 Ω. Therefore, the output voltage is 100*25mA=2.5 V. This 2.5 V is within range of ADC. In Fig. 3.18, first op-amp circuit is voltage follower and the second circuit is for obtaining voltage gain. Here a voltage gain of 2 is used for bringing to 10 V range. Figure 2.13 shows the experimental PCB (Printed

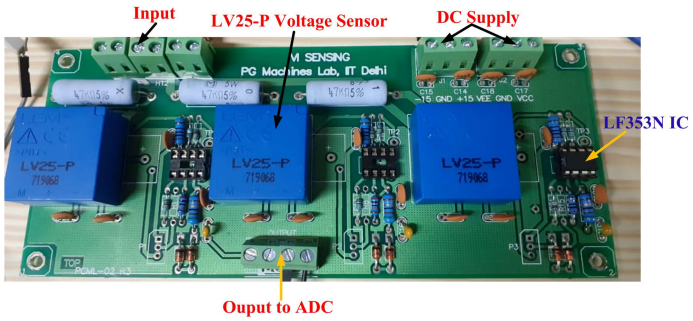

Figure 2.13: Hardware board of voltage sensor PCB

Circuit Board) board of voltage sensor with signal conditioning circuit.

2.7.3 Signal Conditioning Circuit for Hall Effect Current Sensors

VSG and grid currents are sensed using Hall effect current sensors (LEM current sensors, LA55P) and these signals are converted to ±10 V range. Inside the processor, these analog signals are converted into digital signals using ADC and then scaled up to the actual current level inside the processor. The interfacing circuit for converting the actual current into ADC voltage range is shown in Figure 2.14.

The ratings of VSG and grid rms currents are 20A each. In this section, the design of VSG current sensors is discussed. The peak current is 28.28 A ($20 \times \sqrt{2}$). According to the data sheet of the current sensor (LA55P), the primary to secondary conversion ratio is 1:1000. Therefore, the secondary current is 28.28 mA.

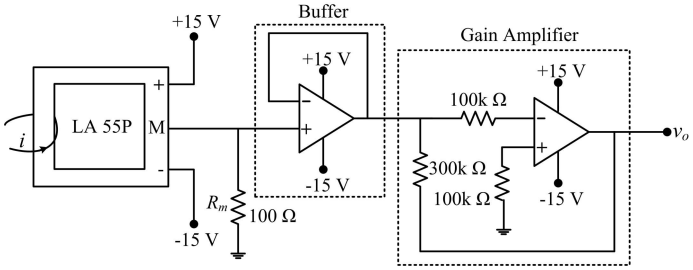

Figure 2.14: Interfacing circuit for current sensor LA 55P

Minimum and maximum measuring resistance according to the data sheet are 50 Ω and 160 Ω. Measuring resistance R_m is selected as 100 Ω. Therefore, the output voltage is 100 Ω × 28.28 mA = 2.828 V. The first op-amp circuit is a voltage follower and the

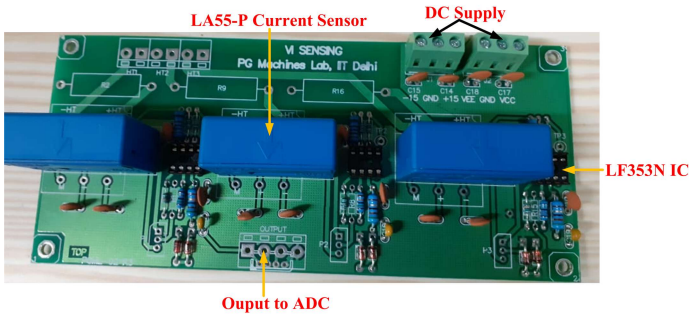

Figure 2.15: Hardware board of current sensor PCB

second circuit is for bringing the signal to the ADC voltage level. For bringing the signal to the ADC voltage of ±10 V, a gain of 3 is attained by the second op-amp circuit. Figure 2.15 shows the photograph of the signal conditioning circuit of the current sensor.

2.7.4 Interfacing Circuit for Opto-Coupler

dSPACE generates the PWM pulses at 5 V logic level. Voltage source inverters (VSIs) module manufactured by Semikron are used in this prototype. This inverter has an internal gate driver. This gate driver needs a voltage level of 15 V for the high logic level. Therefore, there is a need for an external driver circuit to obtain 15 V from the dSPACE logic level of 5 V. This optocoupler is also used as an extra isolation between the processor and the gate driver circuit. The interfacing circuit for the gate driver is shown in Figure 2.16. Here 6N136 IC is used as an optocoupler. The PCB hardware board for the opto-coupler is shown in Figure 2.17.

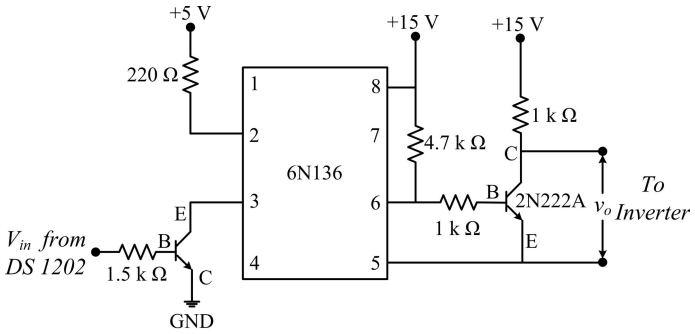

Figure 2.16: Block diagram of optocoupler circuit for the gate driver

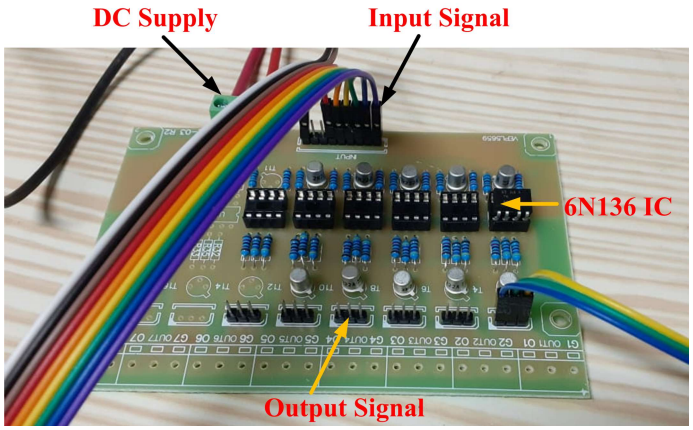

Figure 2.17: PCB board hardware for the opto-coupler

2.8 Hardware results of VSG

This section presents the experimental results of the VSG control algorithm. Experimental results for change in reference active power, change in reference reactive power, and change in reference VSG frequency is discussed in the following subsections.

2.8.1 Change in reference active power

Initially, the active power reference P_m to the grid is increased from 0 to 1 kW, as depicted in Figure 2.18. The active power exchange between VSG and the grid starts occurring, and there is no change in reactive power.

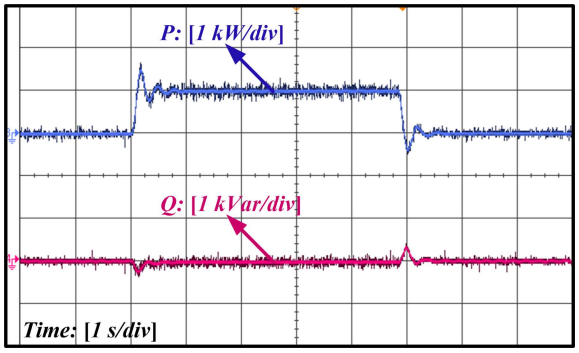

Figure 2.18: Active power response of VSG with change in reference active power

2.8.2 Change in reference reactive power

Now, reactive power reference Q^* to the grid is changed from 0 to 1 $kVar$, assuming that there is no variation in active power reference and frequency. VSG quickly supplies the reactive power Q to track the reactive power command, as shown in Figure 2.19.

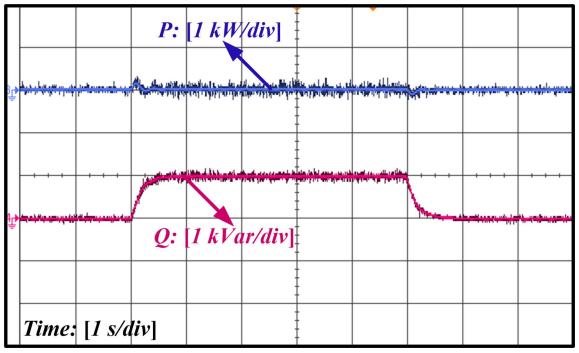

Figure 2.19: Reactive power response of VSG with change in reference reactive power

2.8.3 Change in reference VSG frequency

The behavior of the VSG is observed for frequency regulation by changing the VSG reference frequency. VSG performs the frequency regulation by supplying or absorbing the active power to the grid. The variation of active power generated from VSG when the reference frequency is increased by 0.2 Hz is shown in Figure 2.20.

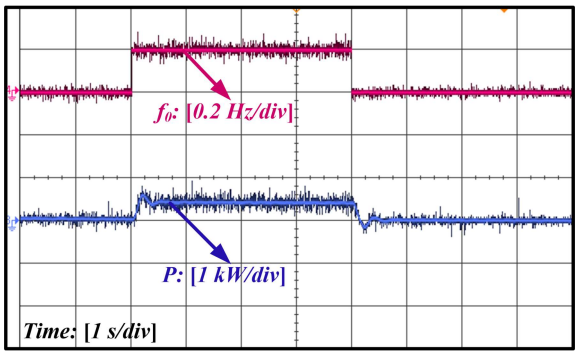

Figure 2.20: Active power response of VSG with change in reference frequency

From Figure (2.18)-(2.20), it is evident that the developed VSG works properly.